

# Hazard, exposure, fragility, and damage state homogenization of a virtual oil refinery testbed for seismic risk assessment

Earthquake Spectra

1–32



© The Author(s) 2024

Article reuse guidelines:

[sagepub.com/journals-permissions](https://sagepub.com/journals-permissions)

DOI: 10.1177/87552930241272521

[journals.sagepub.com/home/eqs](https://journals.sagepub.com/home/eqs)

Vasileios E Melissianos M.EERI<sup>1</sup> , Nikolaos D Karaferis<sup>1</sup>,  
Konstantinos Bakalis<sup>1</sup> , Athanasia K Kazantzi<sup>2</sup>, and  
Dimitrios Vamvatsikos M.EERI<sup>1</sup>

## Abstract

A virtual mid-size oil refinery, located in a high-seismicity region of Greece, is offered as a testbed for developing and testing system-level assessment methods due to direct impact from seismic shaking and without considering geohazards, such as liquefaction and surface faulting. Its characterization is offered in a dedicated repository (<https://doi.org/10.5281/zenodo.11419659>) and it comprises (a) a comprehensive probabilistic treatment of seismic hazard tied to an open-source seismological model; (b) a hazard-consistent set of ground motion records; (c) a full geolocated exposure model with all pertinent critical assets, namely tanks, pressure vessels, process towers, chimneys, equipment-supporting buildings, and a flare; (d) the corresponding record-wise asset demands and summarized fragilities derived via nonlinear dynamic analyses on reduced-order numerical models. Background information is provided on all refinery assets to delineate their role in the refining process. Furthermore, an explicit homogenization of the damage states is proposed, translating them from the asset level to the refinery system level considering the importance of each asset on the overall operational and structural integrity of the refinery. The results can form the basis of any follow-up study that seeks to characterize the effects of cascading failures (fires, explosions), mitigation measures, seismic sequences, and operational constraints on the functionality, risk, and resilience of refining facilities.

<sup>1</sup>Institute of Steel Structures, School of Civil Engineering, National Technical University of Athens, Zografos, Greece

<sup>2</sup>Department of Civil Engineering, School of Engineering, University of Birmingham, Birmingham, UK

## Corresponding author:

Vasileios E Melissianos, Institute of Steel Structures, School of Civil Engineering, National Technical University of Athens, Heron Polytehneiou 9, Polytehneioupoli, 15772 Zografos, Attika, Greece.

Email: [melissia@mail.ntua.gr](mailto:melissia@mail.ntua.gr)

## Keywords

Crude oil refinery, exposure model, virtual testbed, seismic fragility, system impact

Date received: 17 January 2024; accepted: 15 July 2024

## Introduction

Crude oil refining facilities are essential infrastructures for the seamless functioning of a modern society. Crude oil is extracted at onshore and offshore rigs; it is transported via ships and pipelines to crude oil refineries (upstream part) and is then processed to produce liquid and gaseous fuels (midstream part) that are eventually delivered to customers and consumers (downstream part), as shown in Figure 1. The basis of the oil refining process is founded upon the fact that straight-run distillates cannot be directly consumed as fuel due to the high concentration of impurities they contain, and because the octane and cetane numbers are inappropriate for gasoline and diesel engines, respectively (Ancheyta, 2011). Therefore, numerous complex physical and chemical processes are required to deliver the final products. To do so, an oil refinery consists of a variety of assets that are located within a limited area and interact mainly functionally (as opposed to structurally) as they are interconnected via a dense piping network. Thus, the overall health, resilience, and uninterrupted operation of this complex system significantly depend on the structural integrity of its individual assets. As refineries appear to play an important role within the energy supply chain, strict rules, provisions, and guidelines are in effect to ensure their safety and operability, from the design phase up to everyday operation and maintenance activities. However, past earthquake-triggered Natural-Technological (NaTech) accidents, for example, the 1964 Niigata and the 1978 Miyagi earthquakes, Japan (Yoshida, 2014); the 1999 Kocaeli earthquake, Türkiye (Cruz and Steinberg, 2005; Steinberg and Cruz, 2004); the 2003 Tokachi-Oki earthquake, Japan (Hatayama, 2008); the 2010 Bio-Bio offshore earthquake, Chile (Zareian et al., 2012); and the 2011 Great East Japan earthquake (Krausmann and Cruz, 2021), have resulted in devastating consequences for the environment, the economy, and society, thus highlighting the pressing need for more reliable seismic risk estimates in industrial facilities.

While the consensus regarding community-critical infrastructures is that their seismic performance assessment should be carried out on a probabilistic performance basis to account for aleatory and epistemic uncertainties (Cornell and Krawinkler, 2000), research efforts to date are mainly focused on improving the state of knowledge on the seismic performance of individual refinery assets, such as tanks (Bakalis and Karamanos, 2021; Bakalis et al., 2017b; Korkmaz et al., 2011; Vasquez Munoz and Dolšek, 2023; Vathi and Karamanos, 2018), chimneys and process towers (Karaferis et al., 2022), pressure vessels (Karaferis et al., 2024; Wieschollek et al., 2011), building-type structures (Butenweg and Holschoppen, 2014; Butenweg et al., 2021; Kazantzi et al., 2022), and pipe racks (Bursi et al., 2016; Di Sarno and Karagiannakis, 2020). At the same time, the treatment of oil refineries as integrated systems is rather limited, with mostly parts of the petrochemical facilities being investigated in an explicit manner (Farhan and Bousias, 2020; Zhang et al., 2021), while a limited number of qualitative assessment studies have been also carried out (Camila et al., 2019; Cozzani et al., 2014; Krausmann et al., 2019). In more recent studies, associated frameworks to assess the resilience of process plants have been proposed (Caputo et al., 2020; Corritore et al., 2021; Kalemi et al., 2023).

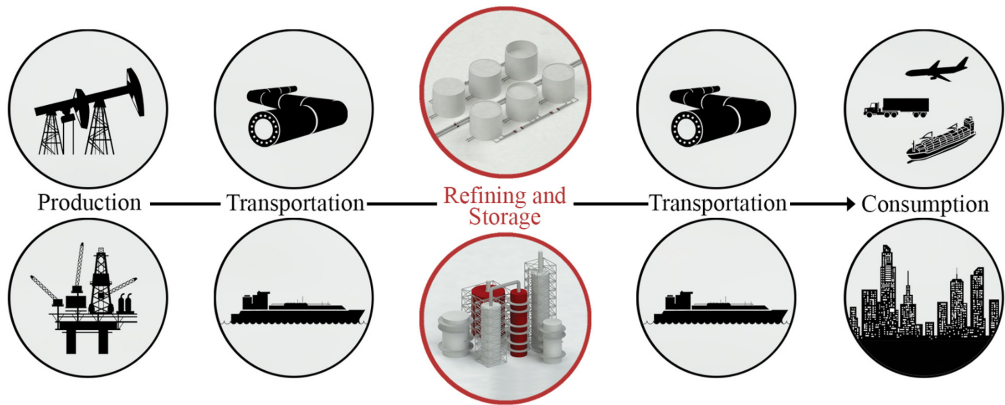


**Figure 1.** The role of oil refineries as a core element in the oil supply chain.

If the above is any indication, refineries are complex and attempting a system-level study carries a steep initial cost. This is the definition of the case study itself, whose details often end up mattering more than any attempted further contribution. Such hurdles have appeared again and again in earthquake engineering. One is reminded of the early Pacific Earthquake Engineering Research (PEER) Center testbeds that helped jump-start performance-based earthquake engineering (Porter, 2003), as well as the more recent example of the Centerville community resilience testbed (Ellingwood et al., 2016) from the Resilience Center. In the same spirit, we aim to offer a virtual refinery testbed with enough information to get researchers started on the system-level assessment.

Specifically, a comprehensive virtual testbed is established for a typical mid-sized crude oil refinery located in a highly seismic area in Greece. It comprises all the needed data to run a quantitative seismic risk assessment up to the level of direct earthquake-induced damages due to seismic shaking, excluding cascading events (e.g. fire and/or explosion). It is noted that earthquake-triggered ground failures (e.g. liquefaction, landslide, faulting) are not considered. The refinery exposure model is developed first, and the critical assets at risk are identified, offering a deeper understanding of the role of each asset in the refining process and their interaction. Seismic hazard analysis results for the area of interest are offered, along with the selection of hazard-consistent records that are utilized to analyze the numerical model of each asset. Seismic fragility curves are extracted and damage states of individual assets are homogenized per their impact at the refinery level to enable a holistic assessment approach. Using these data and results, the basis for enabling the computation of the seismic risk in an oil refinery plant is detailed in the study, providing all the required input and findings thoroughly. The full set of numerical results is offered in the form of spreadsheets in a repository by Melissianos et al. (2024). Additional information such as repair/replacement costs, daily revenue, or amount of oil products processed in the facility is not offered as they are very case-specific, and typically not disclosed by operators.

Overall, one can employ the data provided as a testbed to apply and evaluate the results of different assessment methodologies, testing the effect of simplifications, formulations, discrepancies of concepts, and assumptions involved in assessing the seismic risk of refineries. Using the data provided, one can extricate oneself from tedious structural modeling and analysis and focus on capturing, for instance, the effect of asset correlation, common cause failures, mitigation measures, and the complex phenomena emanating from initial

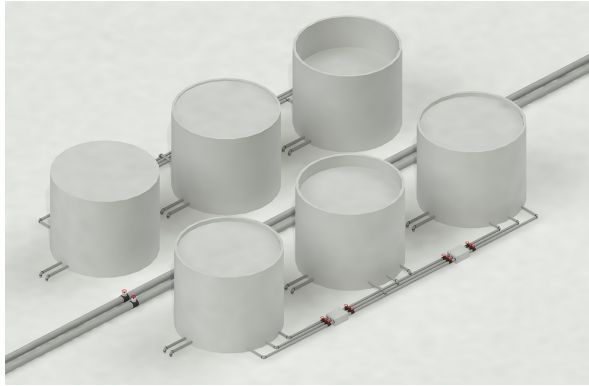


**Figure 2.** Atmospheric liquid-storage steel tanks.

damage, investigating cascading effects and spread of damage due to loss of containment and subsequent fires. On the contrary, the data offered are not suitable for addressing soil-related effects, for example, soil–structure interaction or soil amplification, as the fragilities provided do not incorporate such information.

## Refinery exposure model

A comprehensive list of the main structures typically encountered in an oil refinery is provided in Table 1. In more detail, crude oil (raw material) is imported into the refinery through steel piping, typically buried pipelines of large diameter, and stored in atmospheric liquid storage tanks (see Figure 2). Then, crude oil is refined through numerous chemical and physical processes (i.e. atmospheric distillation, isomerization, catalytic hydrotreating, polymerization and alkylation, fluid catalytic cracking, solvent deasphalting, coking, and so on) in the refining units, which are the core of the facility and include a variety of structures and mechanical equipment. Liquids and gases are continuously circulated in the refining units via a dense steel piping network (see Figure 7). Processes, such as fluid catalytic cracking and vacuum distillation take place in process towers (see Figure 5a). Some other processes, such as heat transfer, take place in mechanical equipment, nested and/or supported by reinforced concrete (RC) and/or steel buildings (see Figure 4). The gases or liquids under pressure required for the refining processes are stored in pressure vessels (see Figure 3b and c). Vapors collected in a closed safety system are disposed of by burning at the refinery flare (see Figure 5c). Gaseous wastes are released in the air via steel and/or RC chimneys (see Figure 5b). Numerous electrical substations (see Figure 6c), which are scattered throughout the refinery, provide the necessary electrical power. Intermediate products of the refining process, such as slope oil, are stored in atmospheric liquid storage tanks (see Figure 2). The final liquid products (marine oil, diesel, gasoline, jet oil, naphtha, asphalt, lubricants, and so on) are stored in atmospheric tanks (see Figure 2), while gases (propane, butane, and so on) in spherical pressure tanks (Figure 3a). Fuel products are exported and supplied to customers via (1) onshore pipelines in the case of very large consumers, such as an airport; (2) road or rail trucks that are loaded at stations (Figure 6a); or (3) ships that moor at piers equipped with dense piping (Figure 6b). Additional structures that are encountered in a refinery comprise control rooms, auxiliary and administrative buildings, cooling towers, and so on.

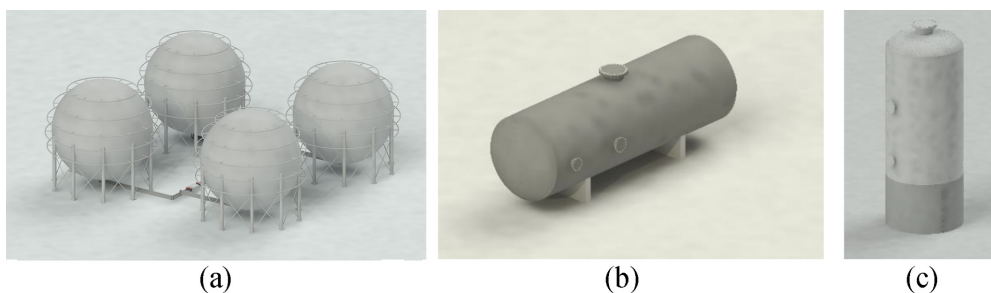


**Figure 3.** Steel pressure vessels: (a) spherical, (b) horizontal, and (c) vertical.



**Figure 4.** (a) Steel and (b) RC equipment-supporting buildings in refining units.

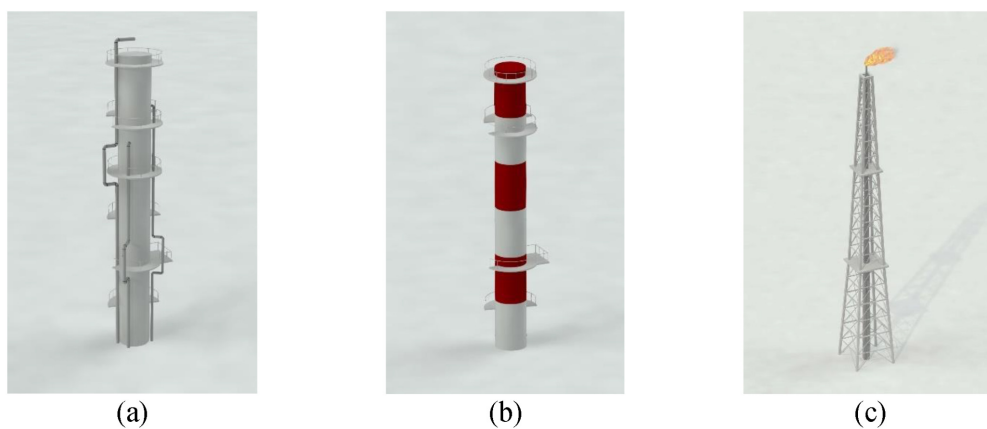


**Figure 5.** High-rise stacks: (a) process tower, (b) steel chimney, (c) flare.

### Virtual refinery testbed

A typical mid-size refinery, in terms of functionality and production, is offered as the VASEL virtual testbed. The refinery plan view is illustrated in Figure 8, covering an area of  $1850 \text{ m} \times 1250 \text{ m}$ . The structures outside the refining unit areas are listed in Table 2,

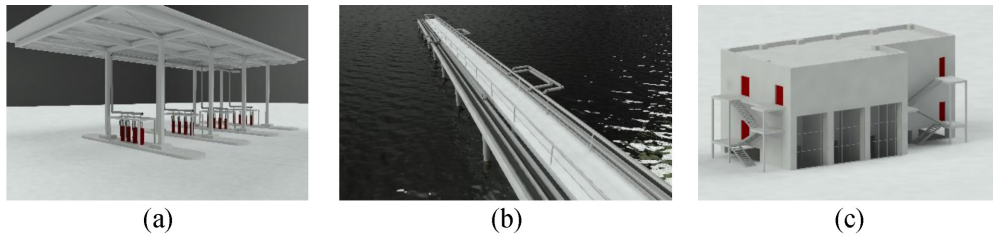


**Figure 6.** Other structures: (a) truck-loading station, (b) pier, (c) electrical substation.

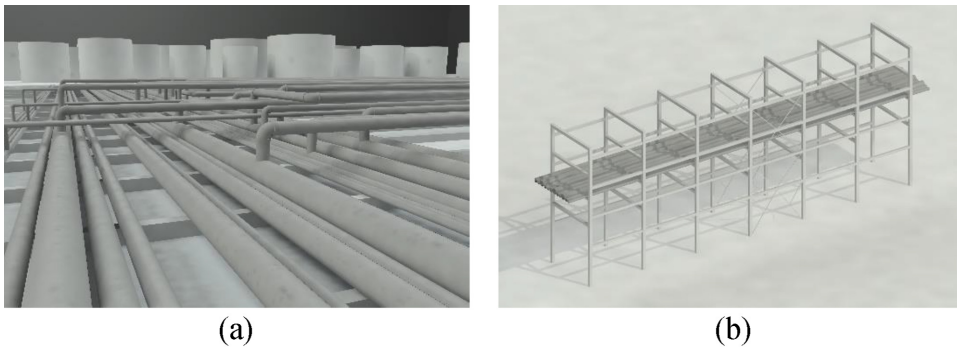


**Figure 7.** Steel piping: (a) above-ground and (b) rack-supported.

**Table I.** List of refinery structures

Structure	Function
Liquid storage tanks	Storage of liquid products (crude oil, gasoline, naphtha, diesel, marine oil, jet oil, and so on; Figure 2)
Pressure vessels	Spherical pressure vessels for storage of final gaseous products (butane, propane, and so on; Figure 3a)
Equipment-supporting buildings	Steel (Figure 4a) and/or reinforced concrete (RC; Figure 4b) buildings that support mechanical equipment and machinery (pressure vessels, heat exchangers, converters, pumps, electrical equipment, and so on)
Process towers	High-rise cylindrical steel stacks (Figure 5a), where physical or chemical processing takes place (e.g. fluid catalytic cracking, distillation, alkylation, and so on)
Chimneys	Steel (Figure 5b) and RC high-rise stacks for the release of gaseous wastes
Pressure vessels	Cylindrical horizontal and vertical pressure vessels for storage of gases used in the refining process (Figure 3b and c)
Flare	Flammable gases and vapors are transported to the top of the high-rise steel lattice tower to be combusted (Figure 5c)
Other structures	Control rooms, auxiliary and administrative buildings, truck-loading station (Figure 6a), pier (Figure 6b), electrical substations (Figure 6c), cooling towers
Piping	Dense network of buried, above-ground (Figure 7a), and rack-supported (Figure 7b) steel piping for oil and gas circulation within the facility

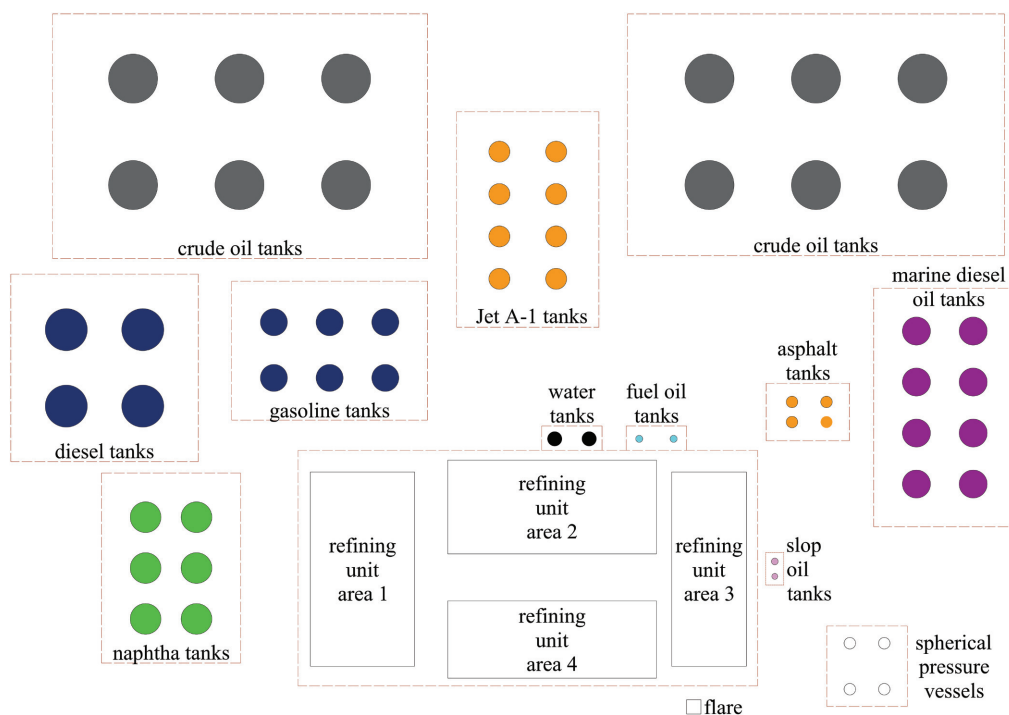


**Figure 8.** Exposure model: plan view of the case study oil refinery.

**Table 2.** Number of individual refinery structures considered in the exposure model

Structure	No.	Structure	No.	Structure	No.
Gasoline tank	6	Naphtha tank	6	Liquid asphalt tank	4
Fuel oil tank	2	Crude oil tank	12	Water tank	2
Marine diesel oil tank	8	Diesel tank	4	Flare	1
Jet A-1 tank	8	Slop oil tank	2	Spherical pressure vessel	4

“No.” denotes the number of structures. Exposure model as shown in Figure 8.

while the structures in the four refining unit areas are listed in Table 3. The exact location of each asset within the refinery stems from the balance between operational optimization and safety provisions (Khor and Elkamel, 2010; Pinto et al., 2000). Some basic principles are the following: (1) the liquid storage tanks cover most of the area and surround the sensitive assets of the facility, namely the refining units, (2) the spherical pressure vessels are located on the seaside or close to a mountain and in any case on the opposite direction of a populated area to minimize the effects in case of failure or accident (e.g. plumes, fireballs, heat radiation) to the facility or the surrounding area, and (3) the main refinery flare is typically located outside the refining units area.

It should be noted that some of the structures listed in Table 1 were not explicitly considered in the analysis, thus missing from Tables 2 and 3, as discussed below:

**Table 3.** Aggregate number of structures in the four refining unit areas considered in the exposure model

Structure	No.	Structure	No.	Structure	No.
One-story RC building	3	Process tower	5	Horizontal pressure vessel	8
Two-story RC building	17	30 m steel chimney	3	Vertical pressure vessel type CL1	12
Four-story RC building	7	80 m steel chimney	1	Vertical pressure vessel type CL2	8
One-story steel building	10	RC chimney	1		
Two-story steel building	9				

“No.” denotes the number of structures. Exposure model as shown in Figure 8.  
RC: reinforced concrete.

- Control rooms are typically heavily overdesigned to additionally serve as bunkers in case of an accident, thus seismic-induced damages are unlikely.
- Auxiliary and administrative buildings, as well as truck loading stations, are designed with increased safety factors. The potential damage or partial failure of these structures is not anticipated to contribute to a NaTech event.
- Piers of marine oil terminals are vulnerable primarily to seismic-induced permanent ground displacements, such as those caused by liquefaction (Goel, 2022; Huang and Han, 2020), and are thus not examined herein.
- Buried steel piping mainly consists of straight segments, that may be damaged due to transient ground displacements caused by seismic wave propagation under specific circumstances related to the soil stratigraphy (Psyrras et al., 2019; Psyrras and Sextos, 2018). Uniform soil conditions have been assumed for the purpose of the testbed and consequently the failure of buried pipes due to seismic wave propagation has been excluded from the scope of work. It should be noted that the buried piping network of the refinery is not directly analogous to an urban gas distribution network since the latter extends over a greater (city-level) area with varying geological conditions and, thus is more vulnerable to seismic-induced permanent and transient ground displacements (Farahani et al., 2020; Kurtuluş, 2011; O’Rourke et al., 2014).
- Above-ground piping is typically attached to sleepers with or without pendulum-type connectors, while expansion joints, U-type pipe loops, elbows, and bends provide the required flexibility for piping thermal expansion and contraction. The two latter conditions tend to be more prevalent where pipe damage is concerned. These configurations along with the piping’s inherent flexibility allow the piping system to undergo slight transverse and longitudinal displacements, thus at most times safely accommodating those imposed by the ground shaking.

It is worth mentioning that although aspects, such as (1) structural interconnectivity (Zhang et al., 2021); (2) local failures of the piping systems, for example, pipe-to-tank connections (O’Rourke et al., 2008; Vathi et al., 2017); (3) failure of piping components (Hosseini et al., 2020); and (4) global failure of the piping systems (Bursi et al., 2015) are not considered in our analysis, as their impact on the seismic risk is expected to be nontrivial and needs to be further investigated. The same applies for the pipe racks, which are open-frame steel (non-building) structures with versatile configuration (Xu et al., 2020). It has been identified after past earthquake events that pipe racks may not be the most vulnerable structures (Krausmann et al., 2010; Paolacci et al., 2012). Still, the potentially critical pipe racks (based on engineering judgment and expert opinion) should be accounted



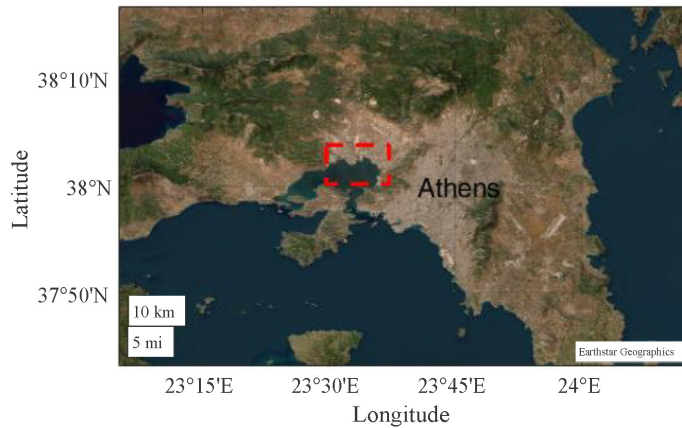


**Figure 9.** Case study area: a major industrial area (marked with a red rectangle) located west of Athens, Greece.

for in a case-specific study. The interested reader may find more information in recent studies (Bedair, 2015; di Sarno and Karagiannakis, 2020a, 2020b) that tried to shed more light on the seismic performance of pipe racks. Finally, the power system (Brennan and Koliou, 2021; Koliou et al., 2013; Oliveto and Reinhorn, 2018; Xie et al., 2019), the water and steam distribution network (Vathi et al., 2017), and transportation networks and their interconnectivity with the refinery structures are not included in the exposure model.

## Seismic hazard

The examined refinery is assumed to be located within a major industrial area, in the west of Athens, Greece (see Figure 9). The OpenQuake engine (Pagani et al., 2014), developed by the Global Earthquake Model Foundation, was employed to compute the seismic hazard in the area of interest. The hazard calculations were based on the results of the 2013 European Seismic Hazard Model (Woessner et al., 2015), for simplicity employing only the area source model and the ground motion prediction equation of Boore and Atkinson (2008) for the site at longitude 23.507 and latitude 38.04. It is noted that the seismic hazard at the area of interest is dominated by the Corinth Gulf faults to the south–southwest, with shallow crustal events having been recorded within a few kilometers of the site. The Hellenic Arc subduction zone is located much further to the south and, although it can produce larger magnitude events, the closest point to the site of interest is at such a horizontal distance ( $\sim 55$  km) and depth ( $\sim 80$  km) that the Arc’s contribution to the short/moderate period hazard is insignificant. For instance, a highly rare “nearby” M8 event on the Hellenic Arc would result in median peak ground accelerations (PGAs) of the order of 0.02–0.04 g, when the 475-year value is an order of magnitude higher at 0.32 g and the 2475-year value reaching 0.60 g (Danciu et al., 2021; Pitilakis et al., 2024). Thus, only the shallow crustal events are considered henceforth.

The seismic intensity measure (IM) serves as an interface variable between seismic hazard and structural analysis and should be a good predictor of the engineering demand parameter (EDP) utilized for the assets under investigation (Kohrangi et al., 2023; Luco and Cornell, 2007). To satisfy this requirement for the various structural typologies that are encountered in an oil refinery, two scalar IMs were employed, namely the *PGA* and

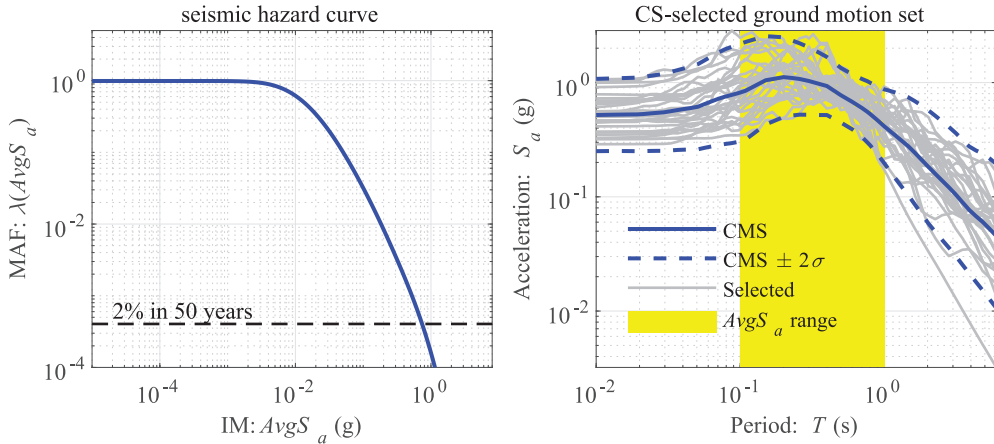


**Figure 10.** Hazard curve: mean annual frequency of exceeding  $AvgS_a$  values (Left); CS-selected ground motion set (Right).

the average spectral acceleration [ $AvgS_a$  (Cordova et al., 2000; Eads et al., 2015; Kazantzi and Vamvatsikos, 2015; Vamvatsikos and Cornell, 2005)].  $PGA$  is an asset-agnostic IM (Karaferis et al., 2022) and was defined herein as the geometric mean of the  $PGA$  values in the two horizontal components of the utilized recorded ground motion records.  $AvgS_a$  is an (moderately) asset-aware IM (Karaferis et al., 2022) and is defined herein as the geometric mean of the spectral accelerations evaluated for both principal horizontal directions within a range of periods. The selected range of periods spans from 0.1 to 1.0 s in increments of 0.1 s. The adopted period range accounts for the vibration periods that are encountered in the majority of the oil refinery structures. It should be underlined that, in general, the optimum—in terms of efficiency—spectral-based IM for each structure is different from the one that was considered herein. However, for a portfolio of structures with considerably different geometry and dynamic characteristics, as in the case of a refinery plant, using more structure-specific IMs [e.g.  $S_a(T_1)$ ] for each one of the considered assets would have resulted in a rather complex and impractical risk assessment framework for the entire facility. In this case, event-based probabilistic seismic hazard analysis involving cross-correlated hazard products would be required, involving correlation relationships among the different IMs (or more accurately the IM residuals per ground motion prediction equation), thus introducing unnecessary complexity.

A set of 30 hazard-consistent natural ground motion records was selected for estimating the structural demands through response-history analysis. The ground motion records were both non-pulse-like and non-long-duration, and were selected from the NGA-West2 database (Ancheta et al., 2013) using the conditional spectrum (CS)-based method reported by Kohrangi et al. (2017, 2018). The set of records corresponds to a probability of exceedance equal to 2% in 50 years (see site hazard curve in Figure 10) that best matches with the CS target (see CS-selected ground motion set in Figure 10). More details on the process of selecting the ground motion records are available in the studies by Bakalis et al. (2018) and Karaferis et al. (2022). In general, to achieve near-optimal hazard consistency, one would require multiple such sets of ground motions selected to correspond to the spectral targets at different levels of each IM. Still, a single hazard-consistent set selected at a critical intensity level of a good IM is typically a good enough

approximation (Kohrangi et al., 2020). It is noted that uniform soil conditions were assumed throughout the limited footprint (approximately 1.8 km × 1.2 km) of the case-study refinery facility, allowing to neglect any kind of ground motion spatial variability. Thus, each ground motion record was applied as is to all refinery assets.

## Fragility analysis background

The typical path for assessing the seismic risk of a structure or infrastructure involves the evaluation of its seismic fragility, which is essentially a metric of the susceptibility of the structure to seismic damage. The computation of the analytical fragility curves is a well-established process (Bakalis and Vamvatsikos, 2018; Baker, 2015; Chatzidaki and Vamvatsikos, 2021; Dymiotis et al., 1999; Kazantzi et al., 2011; Kwon and Elnashai, 2006; Silva et al., 2019). The formal definition of fragility is as follows:

$$F_{LS}(IM) = P[LS \text{ violated} | IM] = P[D > C_{LS} | IM] \quad (1)$$

where  $F_{LS}$  is the cumulative distribution function (CDF) of its argument,  $D$  is the EDP demand, and  $C_{LS}$  is the EDP capacity threshold paired to a specific limit state (LS). The exceedance of the EDP capacity threshold triggers the LS violation and brings the structure into a higher damage state. It is noted that structure-specific damage states are denoted in this study as “ds” to make an essential distinction between them and the global ones referring to the entire facility, denoted as “DS”. The pairing between structure-specific “ds” and global “DS” (termed “homogenization” of damage states) is offered later in the study. It is noted that the use of uppercase and lowercase letters for the damage states only serves to distinguish the refinery- and asset-level damage states, respectively.

In an attempt to strike a balance between accuracy and reduced computational effort (Fragiadakis et al., 2015), the data required to generate fragility functions rely on incremental dynamic analysis [IDA (Vamvatsikos and Cornell, 2002, 2005)] of reduced-order numerical models. The models were developed in the open-source OpenSees platform (McKenna, 1997), and were subjected to the selected set of ground motion records.

## Refinery assets, damage states, and structural models

### Liquid storage tanks

Atmospheric liquid storage tanks are upright cylindrical thin-walled steel structures used to store liquid fuel products. Tanks sit on a very stiff RC foundation and are either anchored to it, typically in the case of high aspect-ratio tanks, or unanchored, in the case of low/moderate aspect-ratio tanks. A set of tanks is considered in the examined refinery, containing raw material (i.e. crude oil), intermediate products (e.g. slope oil), and final products (e.g. kerosene, marine oil, and so on), as presented in Table 2. The considered tanks are listed in Table 4, where tanks TK-2 through TK-10 are unanchored (no physical connection between the structure and its foundation), while tanks TK-13 through TK-16 are anchored (anchor bolts connect the tank shell to the foundation).

The tanks were numerically analyzed by employing the reduced-order model developed by Bakalis et al. (2017a), which is capable of capturing not only the response of tanks supported by anchor straps but also the uplift mechanism of unanchored ones. The EDPs that were employed to monitor structural performance, along with their corresponding failure modes are (Bakalis et al., 2017b): (a) the base plate plastic rotation (base plate damage at

**Table 4.** List of liquid storage tanks ( $\rho_f$ : product density)

	ID	Product	$\rho_f$ (kg/m <sup>3</sup> )		ID	Product	$\rho_f$ (kg/m <sup>3</sup> )
Unanchored tanks	TK-2	Gasoline	750 <sup>(1)</sup>	Anchored tanks	TK-13	Slop oil	900
	TK-3	Fuel oil	900		TK-14	Liquid asphalt	960
	TK-5	Marine diesel oil	820 <sup>(3)</sup>		TK-15	Water	1000
	TK-6	Jet A-1	820 <sup>(4)</sup>		TK-16	Liquid asphalt	960
	TK-8	Naphtha	760				
	TK-9	Crude oil	890 <sup>(5)</sup>				
	TK-10	Diesel	845 <sup>(2)</sup>				

Product density references: <sup>(1)</sup> EN 228:2012 + A1:2017 Automotive fuels. Unleaded petrol. Requirements and test methods, <sup>(2)</sup> EN 590:2023 Automotive fuels—Diesel—Requirements and test methods, <sup>(3)</sup> ISO 8217 “Petroleum Products—Fuel (class F)”, <sup>(4)</sup> IATA Guidance Material (Kerosene Type), NATO Code F-35, <sup>(5)</sup> ISO 12185:1996 Crude Oil and Petroleum Products—Determination of Density—Oscillating U-Tube Method

the wall-to-base connection), (b) the yielding or fracture of the anchor bolts (anchorage failure), (c) the maximum convective wave height of the freeboard (sloshing damage to upper shell course), and (d) the meridional shell stress (elephant’s foot buckling). The four DSs considered for the anchored and the unanchored tanks are summarized in Table 5 along with the associated EDPs, with consequences ranging from no damage to loss of containment. While damage states per individual component (a)–(d) are sequential (e.g. minor versus major damage to the upper shell course), the four overall damage states are nonsequential (Bakalis, et al., 2017b) and to some extent “simultaneous” per FEMA P-58 (2012) parlance, implying that a tank may progress directly to a severe damage state without necessarily sustaining earlier and lower damage associated with a less severe state.

The amount of fuel that is stored in liquid storage tanks is a governing parameter concerning their seismic response (Bakalis et al., 2017a); it is typically expressed through the fill ratio  $FR$ , that is, the ratio of the liquid height to the tank shell height (Bakalis et al., 2017b). Three indicative  $FR$ s are presented herein, namely 0.35, 0.65, and 0.95, featuring the cases of a rather empty tank, a moderately filled one, and a near-full one, respectively. Owing to the above, each  $FR$  corresponds to a different structural response and behavior, and consequently, a separate set of data is included in the dedicated repository. The effect of  $FR$  is presented indicatively for the fuel tank TK-3 in Figure 11 in terms of fragility curves, revealing that the more liquid contained in the tank, the more vulnerable it becomes.

### Equipment-supporting buildings

Various mechanical equipment, such as heat exchangers, vessels, reactors, and so on are installed in building-type structures that are located within the refining unit areas. These assets are either steel or RC open-frame structures (see Figure 4), and typically are heavily overdesigned for fire-proofing. Five typical buildings are examined herein, namely a one-story RC building (ID: RC1), a two-story RC building (ID: RC2), a four-story RC building (ID: RC3), a one-story steel building (ID: ST1), and a two-story steel building (ID: ST2), which were adopted from the study of Kazantzi et al. (2022). More details on the geometry and dynamic properties of the structures, as well as the properties of the supporting equipment, are provided in the repository (Melissianos et al. 2024).

**Table 5.** Liquid storage tank: damage state classification and associated EDPs

Tank	DS	Attainment of DS when	EDP
Anchored	ds0	—	—
	ds1	Minor damage to upper shell course OR Anchorage bolt yielding	Sloshing wave height Anchorage displacement
	ds2	Major damage to upper shell course OR Anchorage bolt fracture OR Minor base plate failure	Sloshing wave height Anchorage displacement Base plate plastic rotation
	ds3	Elephant's foot buckling OR Major base plate failure	Meridional shell stress Base plate plastic rotation
Unanchored	ds0	—	—
	ds1	Minor damage to upper shell course	Sloshing wave height
	ds2	Major damage to upper shell course OR Minor base plate failure	Sloshing wave height Base plate plastic rotation
	ds3	Elephant's foot buckling OR Major base plate failure	Meridional shell stress Base plate plastic rotation

Source: Adapted from Bakalis et al. (2017b).

DS: damage state; EDP: engineering demand parameter.

**Table 6.** Equipment-supporting building: DS classification and associated EDPs for drift-sensitive structural and non-structural components

DS	Attainment of DS when	EDP
ds0	—	—
ds1	Exceedance of interstory drift limit associated with slight damage	Interstory drift ratio
ds2	Exceedance of interstory drift limit associated with moderate damage OR Damage to vertical piping spanning across different stories	Interstory drift ratio
ds3	Exceedance of interstory drift limit associated with near-collapse	Interstory drift ratio

Source: Adapted from Kazantzi et al. (2022).

DS: damage state; EDP: engineering demand parameter.

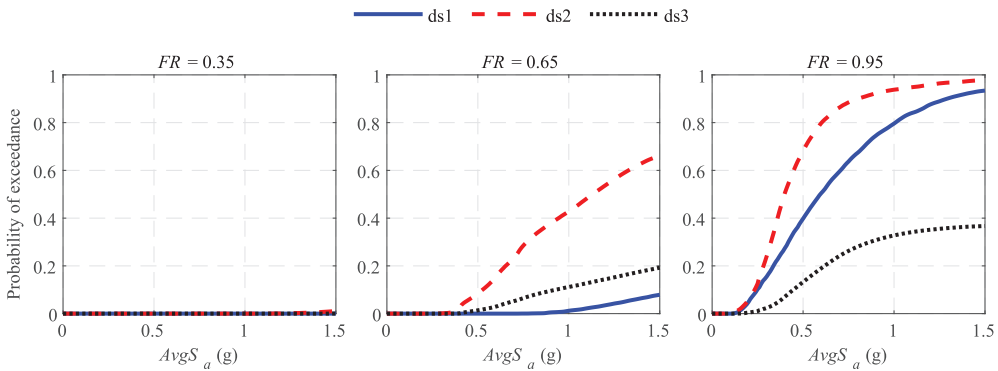
Reduced-order numerical models were developed with elastic beam–column elements and by assigning a rigid diaphragm at the floor levels. Kazantzi et al. (2022) introduced four distinct global DSs with increased severity to assess the seismic performance of these building-type assets. Different DSs were considered for (1) drift-sensitive structural (e.g. columns) and non-structural components (e.g. piping spanning across the building) as shown in Table 6 and (2) acceleration-sensitive components (e.g. reactors, exchangers, and so on) as shown in Table 7. The corresponding DSs are sequential per component, but they are potentially nonsequential at the global level, as some critical equipment may fail catastrophically before the structure attains earlier damage states. In more detail, the interstory drift demands were checked against different drift limits for accessing the seismic performance of the drift-sensitive components, while the seismic acceleration demands on the anchorage points of the acceleration-sensitive components were checked against the corresponding acceleration capacity value (evaluated as the design capacity allowing for an increase due to overstrength). The latter were assigned different importance classes (ICs) to reflect mainly their significance in the refining process and the severity of the consequences in case of a potential failure. Consequently, anchorage failure of the acceleration-sensitive non-structural components that belong to a different IC signifies the attainment of a different damage state.

**Table 7.** Equipment-supporting building: DS classification and associated EDPs for acceleration-sensitive non-structural components

DS	Attainment of DS when	EDP
ds0	—	—
ds1	Anchorage failure of at least one component in IC I	Peak component acceleration
ds2	Anchorage failure of at least one component in IC II	Peak component acceleration
ds3	Anchorage failure of at least one component in IC III	Peak component acceleration

Source: Adapted from Kazantzi et al. (2022).

DS: damage state; EDP: engineering demand parameter; IC: importance class; IC I: low importance equipment; IC II: medium importance equipment; IC III: high importance equipment.

**Figure 11.** TK-3 fuel oil tank: empirical-CDF fragility curves for different fill ratios (FR).

The fragility curves for each building that are provided in the repository have been derived using the “combined component approach” of Kazantzi et al. (2022), tracking damage states per each individual component and employing the correspondence of Tables 6 and 7 to translate local damage states reached into a global DS. Some critical remarks for these curves are the following: (1) drift-sensitive structural and non-structural components are not critical for the seismic performance of the equipment-supporting buildings, since the attainment of all the considered DS due to the damages in the drift-sensitive elements occurs at significantly higher IM levels compared to the acceleration-sensitive non-structural components; (2) the fragility curve of a building associated with a certain DS does not necessarily coincide with the fragility curve of the most vulnerable component belonging to the IC paired with this DS per Table 7; (3) the “combined component” fragility curve denotes the probability of exceeding the acceleration capacity of any component associated with a specific IC, regardless of its location in the floor plan and its elevation. The empirical-CDF fragility curves of the acceleration-sensitive non-structural components for the RC and ST buildings are illustrated in Figure 12. It is observed that the most severe DS3 occurs before DS1 and DS2 for RC1 and RC2 buildings. The latter is attributed to the exceedance of the capacity in many IC III (high importance) equipment, leading to early failure.

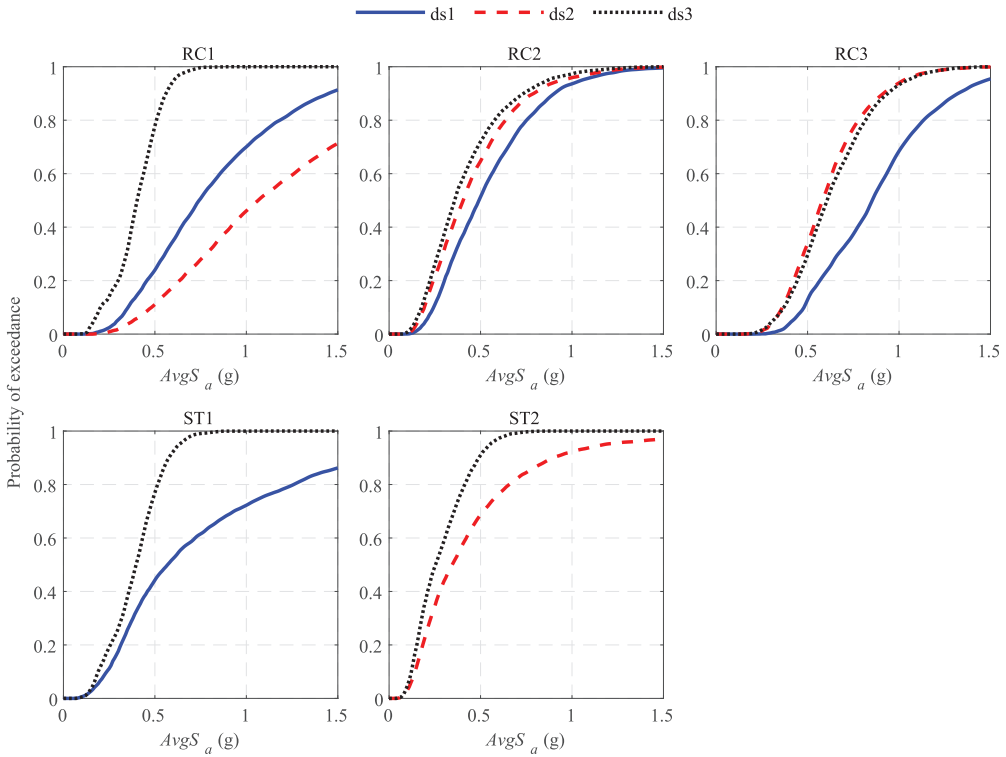


**Figure 12.** RCI-3 and ST1-2 buildings: empirical-CDF fragility curves.

### Process tower

Process towers are tall thin-walled steel structures, where core processes of the refining chain take place, such as atmospheric and vacuum distillation, alkylation, and so on under various levels of internal pressure and temperature. These towers are fixed-based self-supporting slender columns (see Figure 5a). A 30 m high acid settler with an internal diameter equal to 2.6 m is examined, whose geometry and material properties are detailed in the repository. A reduced-order lumped mass numerical model was developed, consisting of concentrated masses at critical elevations along the tower height, connected with elastic beam–column elements. More details on the structure and its modeling can be found in the study by Karaferis et al. (2022). Similar to previous cases, DSs were defined to be sequential per component but potentially nonsequential globally [or “simultaneous” per FEMA P-58] (2012), and they were considered to assess both the operational and the structural seismic performance of the process tower (see Table 8), focusing on the piping and the shell.

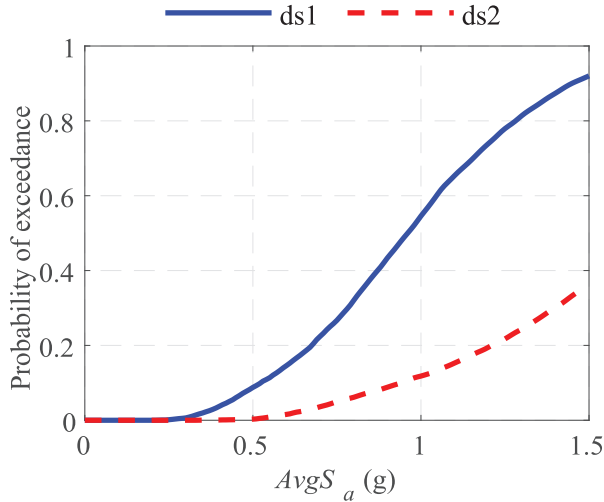
The empirical-CDF fragility curves of the process tower are presented in Figure 13. By inspecting this figure, it can be inferred that for low to moderate earthquake intensity levels up to 0.4 g, the probability of structural damage is insignificant, while for higher levels, there is a non-negligible probability for the tower to see some piping damage (ds1) and lose its operational integrity, without necessarily risking structural collapse (ds2).

**Table 8.** Process tower: damage state classification and associated EDPs

DS	Attainment of DS when	EDP
ds0	—	—
ds1	Damage to connected piping	Top drift
ds2	Local buckling of shell	Shell stress-state

DS: damage state; EDP: engineering demand parameter.

Source: Adapted from Karaferis et al. (2022).

**Figure 13.** Process tower: empirical-CDF fragility curves.

## Chimneys

Chimneys are tall hollow tubular structures used for the disposal of gaseous wastes from the refining process. From a structural point of view, chimneys are essentially self-supporting vertical cantilever beams, which are primarily vulnerable to wind hazard. Still, seismic-related damage to a chimney can occur, especially at the more vulnerable base, and it is expected to obstruct the refining process.

Three typical chimneys are examined in the VASEL testbed, that is, a 30 m and an 80 m high steel chimney (see Figure 5b) as well as an 87 m high RC chimney. These structures have been thoroughly studied by Karaferis et al. (2022) and more details on their geometry and material properties are given in the corresponding spreadsheets in the repository (Melissianos et al., 2024). The chimneys were numerically analyzed using a reduced-order lumped mass model, similar to the one utilized for the process tower. An elastic model was employed for the steel chimneys. For the case of the RC chimney, the elements connecting the concentrated masses were defined as nonlinear forced-based beam–column fiber section elements to account for the steel reinforcement and the concrete material properties. To capture material nonlinearity, the stress–strain model by Mander et al. (1988) was employed for concrete, while an elastic-hardening model with 1% post-hardening stiffness ratio and bounded ductility was used for the reinforcing steel.



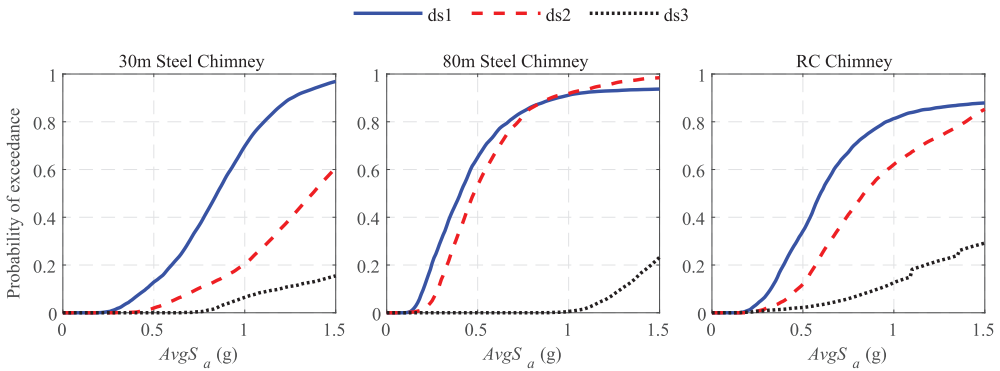


**Figure 14.** Chimneys: empirical-CDF fragility curves.

**Table 9.** Chimney DS classification and associated EDPs

Chimney	DS	Attainment of DS when	EDP
Steel	ds0	—	—
	ds1	Damage to connected piping	Top drift
	ds2	Damage to liner	Interstory drift
	ds3	Local buckling of shell	Shell stress-state
RC	ds0	—	—
	ds1	Damage to connected piping	Top drift
	ds2	Damage to liner or cross-section yielding	Interstory drift or cross-sectional moment
	ds3	Cross-section failure	Cross-sectional moment

Source: Adapted from Karaferis et al. (2022).

DS: damage state; EDP: engineering demand parameter; RC: reinforced concrete.

Four distinct DSs were defined to evaluate the potential damage to the connected piping, the liner, and to assess the stability of the structure itself. Damage is sequential per component, but nonsequential globally. The DS classification and capacity thresholds for the steel and RC chimneys are listed in Table 9. The obtained empirical-CDF fragility curves are shown in Figure 14, where for the steel chimneys we observe that the taller one is more susceptible to both operational disruption (attainment of ds1) and structural damage (attainment of ds2 or ds3), while in both cases the damage states are sequential. The RC chimney has a low probability of catastrophic failure (i.e. reaching ds3 due to cross-section failure) but is more prone to non-structural and minor structural damages, which could undermine its operational continuity.

## Flare

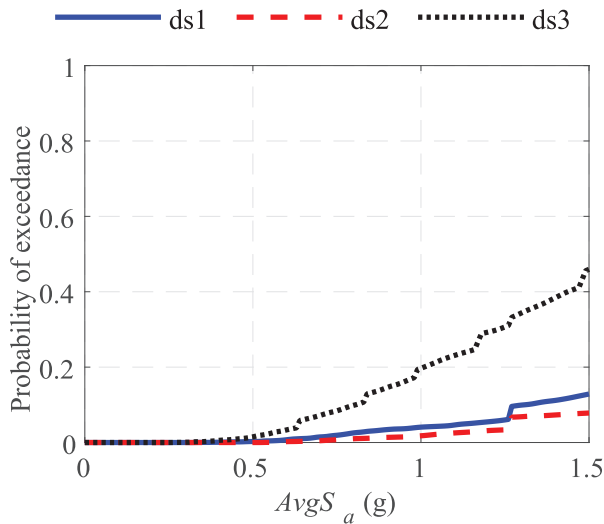
The main flare (see Figure 5c) is the landmark structure in each oil refinery. It is a device for the combustion of regulated vent steams and non-routine emissions resulting from leaks, purges, emergency releases, and so on from the refining process (RTI International, 2015). A network of piping and equipment collects these wastes and transports them to the top of the flare stack to be burned (Bahadori, 2014). From a structural point of view, the flare stack is typically a steel lattice tower that supports the vertical piping and the

**Table 10.** Flare: damage state classification and associated EDPs

DS	Attainment of DS when	EDP
ds0	—	—
ds1	Damage to equipment	Top drift
ds2	Damage to vertical piping	Intersegment drift
ds3	Tensile or buckling structural member failure	Forces and moments of structural members

Source: Adapted from Karaferis et al. (2022).

DS: damage state; EDP: engineering demand parameter.

**Figure 15.** Flare: empirical-CDF fragility curves.

combustion device at the top of the tower. If its operation is disturbed or its structural integrity is endangered due to the occurrence of an earthquake event, the consequences may be far from trivial. This is because in the case of low damage, the refining process may be disrupted, while in the case of major damage, fire or explosion can occur due to the hazardous gases transported within the piping.

A 67.4 m high flare stack is examined for the testbed refinery, consisting of a steel lattice tower with members (legs, diagonals, horizontal) made of circular hollow sections. The structure has been thoroughly investigated by Karaferis et al. (2022) and more details on the geometry and the assumed material properties are provided in the repository (Melissianos et al., 2024). A reduced-order numerical model was developed to analyze the structure. All members were modeled using nonlinear force-based beam–column elements with fiber sections, following the modeling technique for steel lattice towers proposed by Bilonis et al. (2022).

Four distinct damage states (see Table 10) were defined to examine the potential damage to mechanical equipment due to excessive top displacement of the tower, to the vertical piping spanning along the tower height due to excessive intersegment drift, and to the tower itself due to tensile or buckling failure of a member causing catastrophic failure of the structure. Damage states are sequential per component, but nonsequential globally.

**Table 11.** Spherical pressure vessels: damage state classification and associated EDPs

DS	Attainment of DS when	EDP
ds0	—	—
ds1	First yielding of any brace in tension	$d_v \geq 0.063$ m
ds2	Yielding of more than 50% of braces in tension	$d_v \geq 0.091$ m
ds3	Fracture of any brace	$d_v \geq 0.171$ m

Source: Adapted from Karaferis et al. (2024).

DS: damage state; EDP: engineering demand parameter.

The empirical-CDF fragility curves obtained from the analysis are depicted in Figure 15 for both IMs that are considered in this study. It can be inferred that the most critical state is ds3 across the investigated *IM* range, implying that the potential for structural failure is much higher than the potential for operational damages that are depicted through ds1 and ds2. This is an outcome that can be partially attributed to the high stiffness of the tower, which makes it difficult to reach the top and intersegment limits adopted as capacity thresholds for ds1 and ds2, respectively, as well as to the limited redundancy of the flare against individual member failures.

### Spherical pressure vessels

Spherical pressure vessels (Figure 3a) are used in refineries for the storage of liquefied petroleum gases, such as propane, butane, butadiene, isobutylene, and mixtures thereof. These steel spherical vessels are elevated and supported by steel legs of circular hollow sections either equipped with X-bracing or not. Spherical vessels are vulnerable to earthquake-induced damages due to the elevated concentrated mass, especially when fully filled, as revealed in the aftermath of past seismic events (Li et al., 2015).

The considered tank consists of a 20.22 m diameter sphere that is supported by 12 columns with X-bracing and the height to the equator is equal to 13.63 m (Moschonas et al., 2014), while more details on the geometry and the material properties used can be found in the repository (Melissianos et al., 2024). The reduced-order numerical model of Karaferis et al. (2024) was employed to analyze the structure. In more detail, the spherical vessel is simplified to two concentrated masses (Karamanos et al., 2006), that is, the impulsive and the convective components of the fluid mass, the former also containing the mass of the shell. Both are located at the center of the sphere, and connected to the supporting columns via elastic springs and rigid links. The columns are discretized into nonlinear beam-column elements and the braces are modeled with nonlinear truss elements. The basic assumptions of the modeling approach are: (1) the flexibility of the vessel is ignored since any earthquake-induced deformations are anticipated to be much lower than those of the supporting system; (2) the shell is not expected to fail before the supporting system; and (3) the welded connections of the vessel to the columns have sufficient strength. Three sequential damage states were defined to evaluate the structural damage of the tank. The considered EDP is the horizontal displacement ( $d_v$ ) at the center of the sphere (location of the impulsive mass). The damage state classification and capacity thresholds [the latter being case-specific and defined via pushover analysis (Karaferis et al., 2024)] are listed in Table 11.

The amount of gas that is stored in the spherical vessel is expressed by the *FR*, akin to the liquid storage tanks, and determines their seismic response. A range of *FR*s was

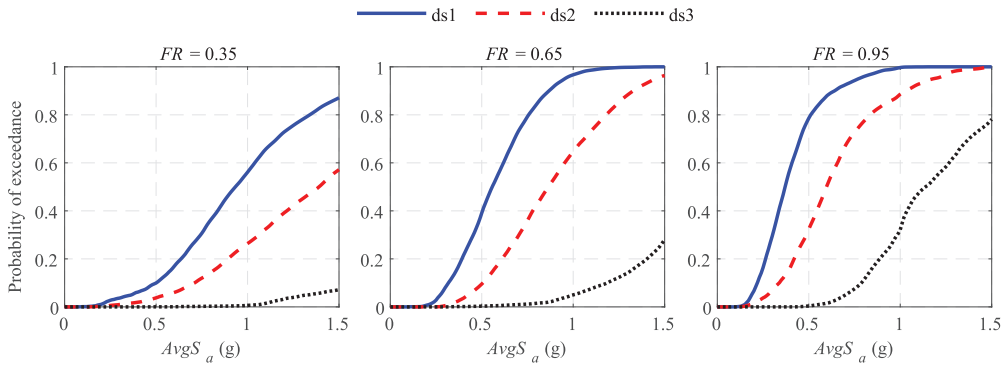


**Figure 16.** Spherical pressure vessels: ensemble empirical-CDF fragility curves for different fill ratios.

considered in the study, from 0.35 to 0.95 with an increment of 0.10. Essentially, each  $FR$  results in a different structure in terms of its dynamic response subject to an earthquake excitation. The effect of the  $FR$  on seismic fragility curves is showcased indicatively in Figure 16 for the three values of 0.35, 0.65, and 0.95, corresponding to a rather empty, a half-filled, and an almost-filled tank, respectively. Results for these  $FR$ s are offered in the repository (Melissianos et al., 2024). It is observed, as expected, that spherical pressure vessels with lower  $FR$ s are less fragile.

### Cylindrical pressure vessels

Numerous horizontal and vertical pressure vessels (see Figure 3b and c) are scattered throughout the refining units for storing the various liquids and gases that are used in the refining process at various temperatures and pressures. Two types of vessels are examined for the VASEL testbed: (a) horizontal cylindrical vessels with steel saddles and vertical rigid supports and (b) vertical cylindrical vessels supported by skirts. These assets have been thoroughly investigated and analyzed by the research team of the European Union-funded research project “PEC—Post-Emergency, Multi-Hazard Health Risk Assessment in Chemical Disasters” and reported in deliverable D.B.1 “Definition of the structural models and seismic fragility analysis techniques available for the specific case study.” The published fragility curves are adopted herein without developing any additional numerical models or undertaking any further analyses. It should be noted that the PEC researchers have carried out their analysis using the  $PGA$  as an IM. Since  $AvgS_a$  is also adopted herein, an IM transformation process was performed through disaggregation of the given fragility curves, using the method presented by Karaferis and Vamvatsikos (2022) to produce fragility curves for  $AvgS_a$  as the IM.

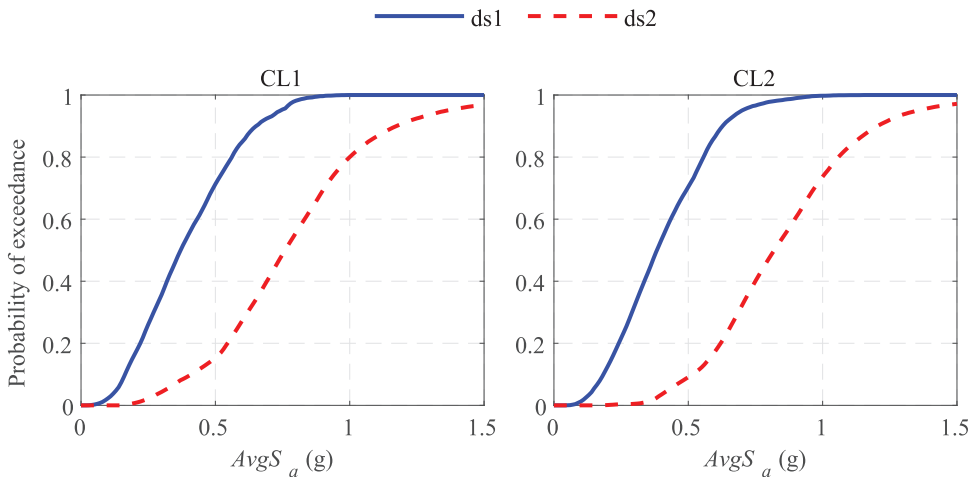
Two categories of vertical pressure vessels were examined by the PEC researchers based on the height-over-diameter ratio ( $H/R$ ), namely, type CL1 for  $4 \leq H/R \leq 7$  and type CL2 for  $7 < H/R \leq 11$ . Following an analysis of the base connection resistance and potential damage to the connected piping due to the vessel’s vertical deformation, two sequential damage states were introduced as listed in Table 12. The fragility curves considered for categories CL1 and CL2 are shown in Figure 17.

The failure of horizontal vessels is attributed to the failure of their anchorage, as has been confirmed by several observations made in the aftermath of past earthquake events

**Table 12.** Vertical pressure vessel: damage state classification and associated EDPs

DS	Attainment of DS when	EDP
ds0	—	—
ds1	First leakage (minor damage to vessel's components)	Rotation of piping and force on base connection
ds2	Complete release of content (failure of piping) and global collapse of vessel (failure of anchorage)	Rotation of piping and force on base connection

DS: damage state; EDP: engineering demand parameter.

**Figure 17.** Vertical pressure vessels of type CL1 and CL2: empirical-CDF fragility curves.**Table 13.** Horizontal pressure vessel: damage state classification and associated EDPs

DS	Attainment of DS when	EDP
ds0	—	—
ds1	First leakage (minor damage to piping) and minor damage to the vessel's structural system	Rotation of piping, base connection, and foundation capacity
ds2	Complete release of content (failure of piping) and global collapse of vessel (failure of anchorage)	Rotation of piping, base connection, and foundation capacity

DS: damage state; EDP: engineering demand parameter.

(Johnson et al., 2000; Roche et al., 1995). Thus, the seismic performance analysis was carried out separately for the longitudinal and the transverse direction of the anchorage concerning the longitudinal axis of the vessel. The anchorage consists of different bolt configurations connecting the saddle to the foundation, with the latter being typically a rigid RC block on the ground level or RC sleepers. Two sequential damage states were introduced related to the performance of the connected piping and the foundation capacity. The damage state classification along with the associated LS definitions are listed in Table 13. The fragility curves considered for the longitudinal and the transverse directions are shown in Figure 18 for  $AvgS_a$ .

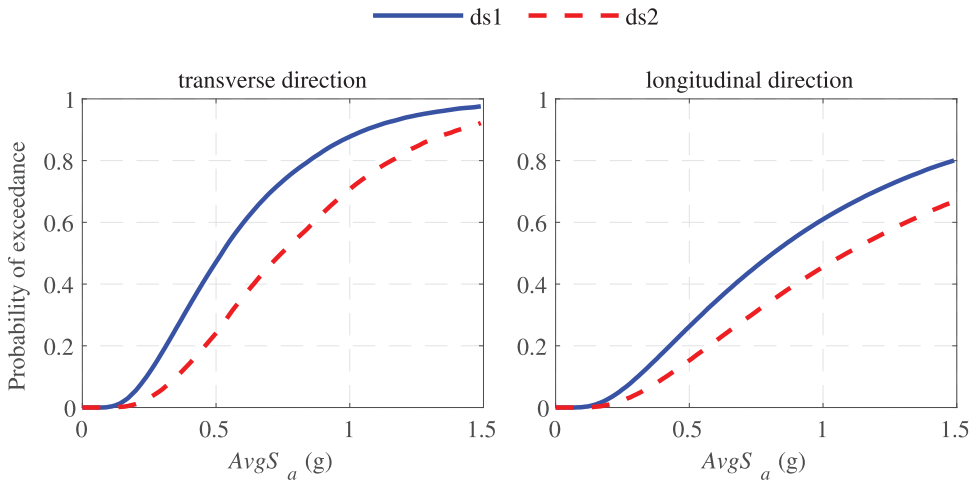


**Figure 18.** Horizontal pressure vessel: empirical-CDF fragility curves in the transverse and longitudinal directions.

Damage State	DS0	DS1	DS2	DS3	DS4
Level of disruption	None	Low	Moderate	Extensive	Severe
Operational status	—	Refinery is operational at almost 100% capacity	Refinery is operational with some parts at reduced capacity	Refinery is partially operational at reduced capacity	Refinery is partially operational at low capacity and may be shut down
Repairs required	—	Some assets require scheduling of minor repairs	Some assets require immediate major repairs	Some assets require extensive repairs	Many assets require extensive repairs and/or replacement

**Figure 19.** Global damage states in terms of operational disruption at the refinery level.

### Homogenization of damage states

Damage states have been identified for each structure separately to examine their susceptibility to damage. However, the failure (either operational or structural) of each asset does not have the same level of impact on the overall operational integrity of the refinery. It is thus useful to homogenize the asset-level damage states (ds) to a set of refinery-level damage states (DS) that better denote their functionality consequences. The latter can be denoted as global DSs and range from “none” to “severe” disruption. The five distinct global DSs are colored after ATC-20 (Applied Technology Council, 1989) and are shown in Figure 19. It is noted that the use of uppercase and lowercase letters for the damage states only serves to distinguish the refinery- and asset-level damage states, respectively.

The homogenization of DSs is offered in Table 14 taking into account the following aspects: (1) the importance of each asset in the refining process, (2) the consequences of potential business disruption (downtime and cost) for the entire refinery, (3) the location of the asset, (4) the potential cascading effects due to a failure and the spread of damage due to loss of containment and subsequent fires, and (5) expert opinion. It should be noted that due to the significant operational interaction between the assets and the complexity of the refining process, the failure of a single asset will have an impact on the refinery's functionality, the magnitude of which depends on a complex combination of factors that cannot be quantified herein.

To offer a deeper understanding of this process, two indicative examples are provided:

- In case a steel chimney fails due to local buckling of the shell (asset-level ds3), the consequences to the refinery would be similarly extensive (refinery-level DS3), as the gaseous waste cannot be released safely. Thus, the part of the refinery that is served by the said chimney needs to cease operations. Note that different chimneys may serve different parts, hence the disruption is somewhat contained. Contrarily, the failure of a steel process tower due to shell local buckling (asset-level ds2) causes a severe functionality reduction (refinery-level DS4) due to this typically being an asset with little-to-no redundancy (for the size of this refinery). Thus, it will directly disrupt the refining process chain, leading to extreme business disruption and downtime until repairs take place.
- In case a vertical or horizontal pressure vessel fails (asset-level ds2), the consequences to the refinery can be considered to be moderate, as different/spare vessels can be employed temporarily. In contrast, the failure of a spherical pressure vessel (asset-level ds3) would have devastating consequences for the entire refinery (severe functionality disruption), considering also the increased potential for fire, explosion, and environmental pollution.

Taking advantage of the homogenization of damage states, it is useful to perform a preliminary qualitative identification of the assets that can contribute most to the disruption of refinery business. To do so, the fragility curves of assets for global DS1 and DS4, indicatively, are shown in Figures 20 and 21, respectively.

It is noted that three indicative liquid storage tanks are presented for illustration purposes, taken as relatively empty ( $FR=0.35$ ), half-full ( $FR=0.65$ ), and almost full ( $FR=0.95$ ). The same  $FR$ s are considered and presented for the spherical pressure vessel. By inspecting the fragilities, it can be seen that: (1) there is significant variability among the assets due to the inherent different dynamic and structural properties; (2) almost full liquid storage tanks and spherical vessels are more susceptible to seismic-induced damage; (3) the potential failure of pressure vessels or the anchorage of acceleration-sensitive equipment nested in buildings or a tall chimney has higher probability to cause low functionality disruption (DS1), compared to other structures; (4) liquid storage tanks that are filled above half of their storage capacity may contribute significantly to severe functionality disruption in comparison to other high-rise stacks or spherical vessels. At this point, it should be noted that the comparison of fragilities offers a preliminary estimation of which asset may fail "first" in case of an earthquake and affect the operation of the refinery. Furthermore, what is critical for the stakeholders is a reliable connection between structural damages and physical consequences (e.g. material release, fire, explosion) in a

**Table 14.** Homogenization of damage states in terms of operational disruption

Structure	DS0 None	DS1 Low disruption	DS2 Moderate	DS3 Extensive	DS4 Severe
Unanchored liquid storage tank	—	ds1: Damage to upper shell course	ds2: Damage to upper shell course or base plate failure		ds3: Exceedance of elephant's foot buckling or base plate failure
Anchored liquid storage tank	—	ds1: Damage to upper shell course or anchorage bolt yielding	ds2: Damage to upper shell course or anchorage bolt fracture or base plate failure		ds3: Exceedance of elephant's foot buckling or base plate failure
Buildings	—	ds1: Anchorage failure of at least one component in IC I	ds2: Anchorage failure of at least one component in IC II	ds3: Anchorage failure of at least one component in IC III	
Process tower	—		ds1: Damage to connected piping		ds2: Local buckling of shell
Steel chimney	—	ds1: Damage to connected piping	ds2: Damage to liner	ds3: Local buckling of shell	
RC chimney	—	ds1: Damage to connected piping	ds2: Damage to liner or cross-section yielding	ds3: Cross-section failure	
Flare	—		ds1: Damage to equipment	ds2: Damage to vertical piping	ds3: Tensile or buckling structural member failure
Spherical pressure vessel	—		ds1: First yielding of any brace in tension	ds2: Yielding of more than 50% of braces in tension	ds3: Fracture of any brace
Vertical pressure vessel	—	ds1: Minor damage of vessel's components	ds2: Failure of piping and global collapse of vessel		
Horizontal pressure vessel	—	ds1: Minor damage to piping and structure	ds2: Failure of piping and anchorage		

DS: damage state; IC: importance class; IC I: low importance equipment; IC II: medium importance equipment; IC III: high importance equipment.



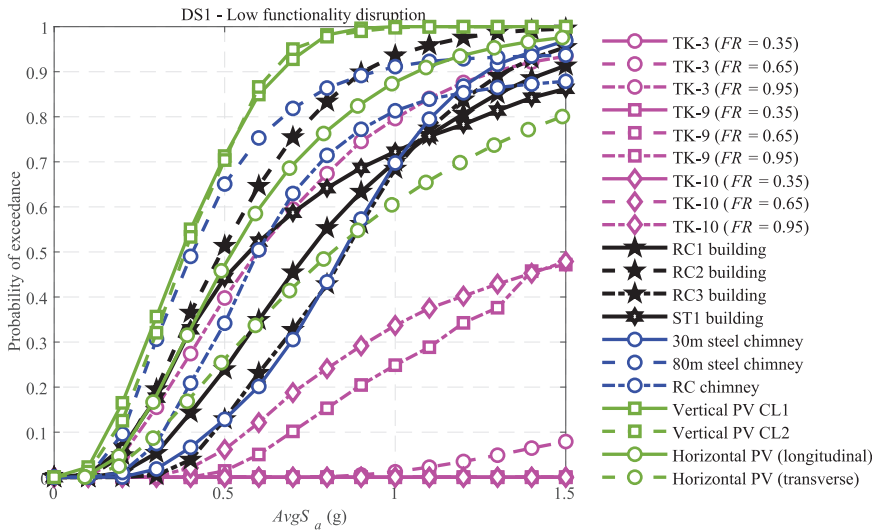


Figure 20. Global DSI: fragility curves of assets.

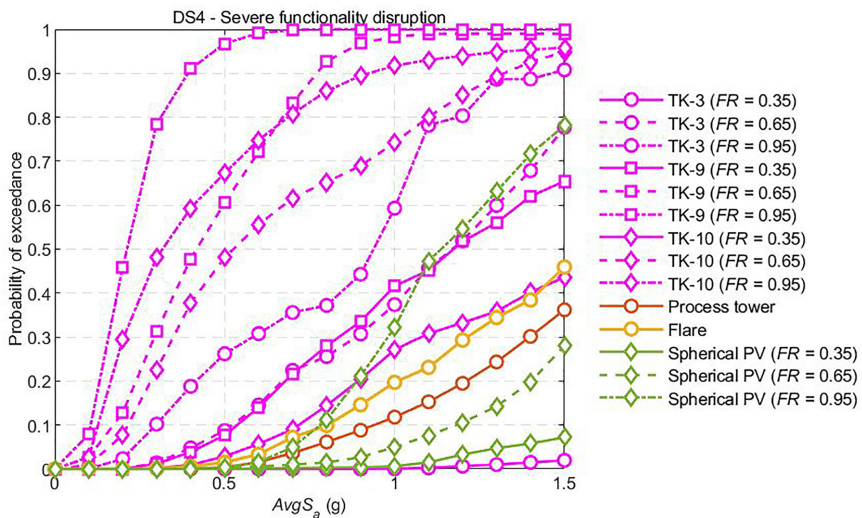


Figure 21. Global DS4: fragility curves of assets.

quantitative manner (Alessandri et al., 2018; Fabbrocino et al., 2005), which is presently out of our scope.

## Repository

The data repository is available by Melissianos et al. (2024) at <https://doi.org/10.5281/zenodo.11419659>. The repository contains separate folders that contain: (a) the seismological data, namely the selected ground motion records and the modified ESHM13 seismological model, (b) the exposure model, and (c) the database related to the refinery assets

examined structured in folders per structural type, namely liquid storage tanks, buildings, pressure vessels, and high-rise stacks. In each folder, a single spreadsheet contains all the information in separate sheets. In more detail: (1) the “Introduction” sheet presents the structure, the nomenclature used, and the contents of the spreadsheet; (2) the “1. Structure” sheet shows the geometry of the asset along with an overview of the developed numerical model; (3) the “2. Modal\_Analysis” sheet presents the results of the structure’s modal analysis in terms of eigenmodes, eigenperiods, and damping ratios, (4) the “3. Damage\_States” sheet shows the considered damage states, along with the EDP and the corresponding capacity checks, (5) the “4.1.\*. IDA\_PGA\_\*\*” and “4.2.\*. IDA\_AvgSa\_\*\*” sheets list the IDA results from both IMs ( $PGA$  and  $AvgS_a$ ) considered per  $EDP$  (\* denotes the number of the  $EDP$  and \*\* denotes its name); (6) the “5.1. Fragility\_PGA” and “5.2. Fragility\_AvgSa” sheets present the calculated empirical-CDF fragilities, which are also plotted for illustration purposes in the “5.3. Fragility\_Plots” sheet.

## Conclusion

In support of seismic risk and resilience assessment of industrial facilities and NaTech events, we present the VASEL virtual testbed, resembling a realistic mid-size refinery in high-seismicity Mediterranean regions. It comprises a full exposure model with site seismic hazard and fragility definition of the critical refinery assets. Critical details for the location and function of each structure are provided, offering earthquake and risk engineers an insight into the facility’s operation and how the operational interdependencies of the assets affect the risk estimation process.

The critical assets at risk are identified and analyzed via appropriate simplified (reduced-order or surrogate) models that can capture the main failure modes associated with functionality disruption and structural damage. High-fidelity fragility curves are produced to identify each asset’s susceptibility to business interruption or structural damage for various levels of seismic intensity. Moreover, critical issues associated with these assets are detailed and demonstrated, such as the importance of equipment supported in building-type structures, how this affects the fragility of the structure, and the effect of the  $FR$  in liquid and gas storage tanks. The homogenization of damages states is presented to showcase the transition from the asset to the refinery level to assess the potential of refinery functionality disruption and associated NaTech events. Finally, a modern refinery remains a complex petrochemical facility for which we have only provided structural information on critical assets. Piping, water, steam, power, and transportation infrastructure, as well as their interconnectivity with the described assets, are required to form a complete picture of the refinery, even in its virtual testbed form.

## Acknowledgments

The authors would like to thank all practitioners who offered information on refinery assets and operations, Ms. E. Vourlakou for producing the schematics and illustrations that appear in this article, and Dr. Akrivi Chatzidaki for performing the seismic hazard analysis.


## Declaration of conflicting interests


The author(s) declared no potential conflicts of interest with respect to the research, authorship, and/or publication of this article.

## Funding

The author(s) disclosed receipt of the following financial support for the research, authorship, and/or publication of this article: This research has been co-financed by the European Union through the HORIZON 2020 research and innovation program “METIS–Seismic Risk Assessment for Nuclear Safety” under Grant Agreement No. 945121 and the HORIZON innovation action “PLOT0–Deployment and Assessment of Predictive modelling, environmentally sustainable and emerging digital technologies and tools for improving the resilience of IWW against Climate change and other extremes” under Grant Agreement No. 101069941.

## ORCID iDs

Vasileios E. Melissianos  <https://orcid.org/0000-0002-1589-0697>

Konstantinos Bakalis  <https://orcid.org/0000-0002-0826-1059>

## Research data and code availability

The open-source data presented in this article is available by Melissianos et al. (2024). [Reference in list: Melissianos VE, Kareferis ND, Bakalis K, Kazantzi AK and Vamvatsikos D (2024) Exposure and fragility of a virtual oil refinery testbed for seismic risk assessment. *Zenodo*. DOI: <https://doi.org/10.5281/zenodo.11419659>]. No specific software was used for the analysis.

## References

- Alessandri S, Caputo AC, Corritore D, Giannini R, Paolacci F and Phan HN (2018) Probabilistic risk analysis of process plants under seismic loading based on Monte Carlo simulations. *Journal of Loss Prevention in the Process Industries* 53: 136–148.
- Ancheta TD, Darragh RB, Stewart JP, Seyhan E, Silva WJ, Chiou BSJ, Wooddell KE, Graves RW, Kottke AR, Boore DM, Kishida T and Donahue JL (2013) *PEER Nga-west2 Database*. Technical Report PEER 2013/03, Berkeley, CA. Available at: [https://apps.peer.berkeley.edu/publications/peer\\_reports/reports\\_2013/webPEER-2013-03-Ancheta.pdf](https://apps.peer.berkeley.edu/publications/peer_reports/reports_2013/webPEER-2013-03-Ancheta.pdf)
- Ancheyta J (2011) *Modeling and Simulation of Catalytic Reactors for Petroleum Refining*. Hoboken, NJ: John Wiley & Sons.
- Applied Technology Council (1989) *ATC-20 Procedures for Postearthquake Safety Evaluation of Buildings*. Redwood City CA. Available at: <https://www.atccouncil.org/atc-20>
- Bahadori A (2014) Blow-down and flare systems. *Natural Gas Processing* 2014: 275–312.
- Bakalis K and Karamanos SA (2021) Uplift mechanics of unanchored liquid storage tanks subjected to lateral earthquake loading. *Thin-walled Structures* 158: 107145.
- Bakalis K and Vamvatsikos D (2018) Seismic fragility functions via nonlinear response history analysis. *Journal of Structural Engineering* 144(10): 04018181.
- Bakalis K, Fragiadakis M and Vamvatsikos D (2017a) Surrogate modeling for the seismic performance assessment of liquid storage tanks. *Journal of Structural Engineering* 143(4): 04016199.
- Bakalis K, Kohrangi M and Vamvatsikos D (2018) Seismic intensity measures for above-ground liquid storage tanks. *Earthquake Engineering & Structural Dynamics* 47(9): 1844–1863.
- Bakalis K, Vamvatsikos D and Fragiadakis M (2017b) Seismic risk assessment of liquid storage tanks via a nonlinear surrogate model. *Earthquake Engineering and Structural Dynamics* 46(15): 2851–2868.
- Baker JW (2015) Efficient analytical fragility function fitting using dynamic structural analysis. *Earthquake Spectra* 31(1): 579–599.
- Bedair O (2015) Rational design of pipe racks used for oil sands and petrochemical facilities. *Practice Periodical on Structural Design and Construction* 20(2): 04014029.

- Bilionis DV, Vlachakis K, Vamvatsikos D, Dasiou M-E, Vayas I and Lagouvardos K (2022) Risk assessment of rehabilitation strategies for steel lattice telecommunication towers of Greece under extreme wind hazard. *Engineering Structures* 267: 114625.
- Boore DM and Atkinson GM (2008) Ground-Motion prediction equations for the average horizontal component of PGA, PGV and 5%-damped PSA at spectral periods between 0.01 s and 10.0 s. *Earthquake Spectra* 24(1): 99–138.
- Brennan AL and Koliou M (2021) Probabilistic loss assessment of a seismic retrofit technique for medium- and high-voltage transformer bushing systems in high seismicity regions. *Structure and Infrastructure Engineering* 17(8): 1036–1045.
- Bursi OS, Paolacci F, Reza MS, Alessandri S and Tondini N (2016) Seismic assessment of petrochemical piping systems using a performance-based approach. *Journal of Pressure Vessel Technology* 138(3): 031801.
- Bursi OS, Reza MS, Abbiati G and Paolacci F (2015) Performance-based earthquake evaluation of a full-scale petrochemical piping system. *Journal of Loss Prevention in the Process Industries* 33: 10–22.
- Butenweg C and Holtschoppen B (2014) Seismic design of industrial facilities in Germany. In: Klinkel S, Butenweg C, Lin G and Holtschoppen B (eds) *Seismic Design of Industrial Facilities*. Wiesbaden: Springer Fachmedien Wiesbaden, pp. 63–74.
- Butenweg C, Bursi OS, Paolacci F, Marinković M, Lanese I, Nardin C and Quinci G (2021) Seismic performance of an industrial multi-storey frame structure with process equipment subjected to shake table testing. *Engineering Structures* 243: 112681.
- Camila S-PM, Perreur M, Munoz F and Cruz AM (2019) Systematic literature review and qualitative meta-analysis of Natech research in the past four decades. *Safety Science* 116: 58–77.
- Caputo AC, Kalemi B, Paolacci F and Corritore D (2020) Computing resilience of process plants under Na-Tech events: Methodology and application to seismic loading scenarios. *Reliability Engineering and System Safety* 195: 106685.
- Chatzidaki A and Vamvatsikos D (2021) Mixed probabilistic seismic demand models for fragility assessment. *Bulletin of Earthquake Engineering* 19(15): 6397–6421.
- Cordova PP, Deierlein GG, Mehanny SSF and Cornell CA (2000) Development of a two-parameter seismic intensity measure and probabilistic assessment procedure. In: *Second U.S.-Japan workshop on performance-based earthquake engineering methodology for reinforced concrete building structures*, Sapporo, Japan, 11–13 September.
- Cornell CA and Krawinkler H (2000) Progress and challenges in seismic performance assessment. *PEER Center News* 3(2): 1–4.
- Corritore D, Paolacci F and Caprinuzzi S (2021) A screening methodology for the identification of critical units in major-hazard facilities under seismic loading. *Frontiers in Built Environment* 7: 780719.
- Cozzani V, Antonioni G, Landucci G, Tugnoli A, Bonvicini S and Spadoni G (2014) Quantitative assessment of domino and NaTech scenarios in complex industrial areas. *Journal of Loss Prevention in the Process Industries* 28: 10–22.
- Cruz AM and Steinberg LJ (2005) Industry preparedness for earthquakes and earthquake-triggered hazmat accidents in the 1999 Kocaeli earthquake. *Earthquake Spectra* 21(2): 285–303.
- Danciu L, Nandan S, Reyes C, Basili R, Weatherill G, Beauval C, Rovida AN, Susana V, Karin S, Pierre-Yves B, Fabrice C, Stefan W and Domenico G (2021) *The 2020 Update of the European Seismic Hazard Model—ESHM20: Model Overview*. EFEHR Technical Report 001 V1.0.0, Zurich.
- Di Sarno L and Karagiannakis G (2020) Petrochemical steel pipe rack: Critical assessment of existing design code provisions and a case study. *International Journal of Steel Structures* 20(1): 232–246.
- di Sarno L and Karagiannakis G (2020a) On the seismic fragility of pipe rack—piping systems considering soil–structure interaction. *Bulletin of Earthquake Engineering* 18(6): 2723–2757.
- di Sarno L and Karagiannakis G (2020b) Seismic assessment of pipe racks accounting for soil–structure interaction. *International Journal of Steel Structures* 20(6): 1929–1944.

- Dymiotis C, Kappos AJ and Chryssanthopoulos MK (1999) Seismic reliability of RC frames with uncertain drift and member capacity. *Journal of Structural Engineering* 125(9): 1038–1047.
- Eads L, Miranda E and Lignos DG (2015) Average spectral acceleration as an intensity measure for collapse risk assessment. *Earthquake Engineering & Structural Dynamics* 44(12): 2057–2073.
- Ellingwood BR, Cutler H, Gardoni P, Peacock WG, van de, Lindt JW and Wang N (2016) The centerville virtual community: A fully integrated decision model of interacting physical and social infrastructure systems. *Sustainable and Resilient Infrastructure* 1(3–4): 95–107.
- Fabbrocino G, Iervolino I, Orlando F and Salzano E (2005) Quantitative risk analysis of oil storage facilities in seismic areas. *Journal of Hazardous Materials* 123(1–3): 61–69.
- Farahani S, Tahershamsi A and Behnam B (2020) Earthquake and post-earthquake vulnerability assessment of urban gas pipelines network. *Natural Hazards* 101(2): 327–347.
- Farhan M and Bousias S (2020) Seismic fragility analysis of LNG sub-plant accounting for component dynamic interaction. *Bulletin of Earthquake Engineering* 18(10): 5063–5085.
- Fragiadakis M, Vamvatsikos D, Karlaftis MG, Lagaros ND and Papadrakakis M (2015) Seismic assessment of structures and lifelines. *Journal of Sound and Vibration* 334: 29–56.
- FEMA. Seismic Performance Assessment of Buildings. 1. FEMA P-58 Washington D.C: Prepared by the Applied Technology Council for the Federal Emergency Management Agency; 2012. <https://femap58.atcouncil.org/documents/fema-p-58/24-fema-p-58-volume-1-methodology-second-edition/file>
- Goel RK (2022) Evaluation of seismic force provisions for nonstructural systems supported on marine structures considering effects of nonlinearity. *Earthquake Spectra* 38(4): 3017–3039.
- Hatayama K (2008) Lessons from the 2003 Tokachi-oki, Japan, earthquake for prediction of long-period strong ground motions and sloshing damage to oil storage tanks. *Journal of Seismology* 12(2): 255–263.
- Hosseini M, Ghalyani E and Ghorbani Amirabad N (2020) Development of double-variable seismic fragility functions for oil refinery piping systems. *Journal of Loss Prevention in the Process Industries* 68: 104259.
- Huang Y and Han X (2020) Features of earthquake-induced seabed liquefaction and mitigation strategies of novel marine structures. *Journal of Marine Science and Engineering* 8(5): 310.
- Johnson GS, Aschheim M and Sezen H (2000) Industrial facilities. *Earthquake Spectra* 16(1\_suppl): 311–350.
- Kalemi B, Caputo AC, Corritore D and Paolacci F (2023) A probabilistic framework for the estimation of resilience of process plants under Na-Tech seismic events. *Bulletin of Earthquake Engineering* 22: 75–106.
- Karaferis ND and Vamvatsikos D (2022) Intensity measure transformation of fragility curves for 2D buildings using simplified models. In: *3rd European conference on earthquake engineering & seismology*, Bucharest, 4–9 September.
- Karaferis ND, Kazantzi AK, Melissianos VE, Bakalis K and Vamvatsikos D (2022) Seismic fragility assessment of high-rise stacks in oil refineries. *Bulletin of Earthquake Engineering* 20(12): 6877–6900.
- Karaferis ND, Melissianos VE and Vamvatsikos D (2024) Mechanical modeling, seismic fragility and correlation issues for groups of spherical pressure vessels. *Acta Mechanica* 235(3): 1563–1582. <https://link.springer.com/article/10.1007/s00707-023-03670-8>
- Karamanos SA, Patkas LA and Platyrrachos MA (2006) Sloshing effects on the seismic design of horizontal-cylindrical and spherical industrial vessels. *Journal of Pressure Vessel Technology* 128(3): 328–340.
- Kazantzi AK and Vamvatsikos D (2015) Intensity measure selection for vulnerability studies of building classes. *Earthquake Engineering & Structural Dynamics* 44(15): 2677–2694.
- Kazantzi AK, Karaferis ND, Melissianos VE, Bakalis K and Vamvatsikos D (2022) Seismic fragility assessment of building-type structures in oil refineries. *Bulletin of Earthquake Engineering* 20(12): 6853–6876.
- Kazantzi AK, Righiniotis TD and Chryssanthopoulos MK (2011) A simplified fragility methodology for regular steel MRFs. *Journal of Earthquake Engineering* 15(3): 390–403.

- Khor CS and Elkamel A (2010) Superstructure optimization for oil refinery design. *Petroleum Science and Technology* 28(14): 1457–1465.
- Kohrangi M, Bakalis K, Triantafyllou G, Vamvatsikos D and Bazzurro P (2023) Hazard consistent record selection procedures accounting for horizontal and vertical components of the ground motion: Application to liquid storage tanks. *Earthquake Engineering & Structural Dynamics* 52(4): 1232–1251.
- Kohrangi M, Bazzurro P, Vamvatsikos D and Spillatura A (2017) Conditional spectrum-based ground motion record selection using average spectral acceleration. *Earthquake Engineering & Structural Dynamics* 46(10): 1667–1685.
- Kohrangi M, Bazzurro P, Vamvatsikos D and Spillatura A (2018) Corrigendum to: Conditional spectrum-based ground motion record selection using average spectral acceleration: Conditional spectrum-based record selection (*Earthquake Engineering & Structural Dynamics*, (2017), 46, 10, (1667-1685), 10.1002/eqe.2876). *Earthquake Engineering and Structural Dynamics* 47(1): 265.
- Kohrangi M, Vamvatsikos D and Bazzurro P (2020) Multi-level conditional spectrum-based record selection for IDA. *Earthquake Spectra* 36(4): 1976–1994.
- Koliou M, Filiatrault A and Reinhorn AM (2013) Seismic response of high-voltage transformer-bushing systems incorporating flexural stiffeners I: Numerical study. *Earthquake Spectra* 29(4): 1335–1352.
- Korkmaz KA, Sari A and Carhoglu AI (2011) Seismic risk assessment of storage tanks in Turkish industrial facilities. *Journal of Loss Prevention in the Process Industries* 24(4): 314–320.
- Krausmann E and Cruz AM (2021) Natech risk management in Japan after Fukushima—What have we learned? *Loss Prevention Bulletin* 277: 10–14. Available at: <https://www.icheme.org/media/15301/krausmannnew.pdf>
- Krausmann E, Girgin S and Necci A (2019) Natural hazard impacts on industry and critical infrastructure: Natech risk drivers and risk management performance indicators. *International Journal of Disaster Risk Reduction* 40: 101163.
- Krausmann E, Maria A and Affeltranger B (2010) The impact of the 12 May 2008 Wenchuan earthquake on industrial facilities. *Journal of Loss Prevention in the Process Industries* 23(2): 242–248.
- Kurtuluş A (2011) Pipeline vulnerability of Adapazari during the 1999 Kocaeli, Turkey, earthquake. *Earthquake Spectra* 27(1): 45–66.
- Kwon OS and Elnashai A (2006) The effect of material and ground motion uncertainty on the seismic vulnerability curves of RC structure. *Engineering Structures* 28(2): 289–303.
- Li X, Koseki H and Sam Mannan M (2015) Case study: Assessment on large scale LPG BLEVEs in the 2011 Tohoku earthquakes. *Journal of Loss Prevention in the Process Industries* 35: 257–266.
- Luco N and Cornell CA (2007) Structure-specific scalar intensity measures for near-source and ordinary earthquake ground motions. *Earthquake Spectra* 23(2): 357–392.
- McKenna, F. 1997. “Object oriented finite element programming frameworks for analysis, algorithms and parallel computing.” Ph.D. dissertation, Dept. of Civil and Environmental Engineering, Univ. of California at Berkeley.
- Mander JB, Priestley MJN and Park R (1988) Theoretical stress-strain model for confined concrete. *Journal of Structural Engineering* 114(8): 1804–1826.
- Melissianos VE, Kareferis ND, Bakalis K, Kazantzi AK and Vamvatsikos D (2024) Exposure and fragility of a virtual oil refinery testbed for seismic risk assessment. *Zenodo*. Available at: <https://zenodo.org/records/11419659>
- Moschonas F, Karakostas C, Lekidis V and Papadopoulos S (2014) Investigation of seismic vulnerability of industrial pressure vessels. In: *Proceedings of the Second European conference on earthquake engineering and seismology*, Istanbul, 25–29 August. Available at: [http://www.eaee.org/Media/Default/2ECCES/2ecces\\_ss/2324.pdf](http://www.eaee.org/Media/Default/2ECCES/2ecces_ss/2324.pdf)
- Oliveto ND and Reinhorn AM (2018) Evaluation of as-installed properties of transformer bushings. *Engineering Structures* 162: 29–36.
- O’Rourke MJ, Symans MD, Masek JP, Rourke MJO, Eeri M and Symans MD (2008) Wave propagation effects on buried pipe at treatment plants. *Earthquake Spectra* 24(3): 725–749.

- O'Rourke TD, Jeon SS, Toprak S, Cubrinovski M, Hughes M, van Ballegooy S and Bouziou D (2014) Earthquake response of underground pipeline networks in Christchurch, NZ. *Earthquake Spectra* 30(1): 183–204.
- Pagani M, Monelli D, Weatherill G, Danciu L, Crowley H, Silva V, Henshaw P, Butler L, Nastasi M, Panzeri L, Simionato M and Vigano D (2014) Openquake engine: An open hazard (and risk) software for the global earthquake model. *Seismological Research Letters* 85(3): 692–702.
- Paolacci F, Giannini R and De M (2012) Analysis of the seismic risk of major-hazard industrial plants and applicability of innovative seismic protection systems. In: Patel V (ed.) *Petrochemicals*. Rijeka: IntechOpen, pp. 223–248.
- Pinto JM, Joly M and Moro LFL (2000) *Planning and Scheduling Models for Refinery Operations*. *Computers and Chemical Engineering*. *Artigo de periodico* 24: 2259–2276.
- Pitilakis K, Riga E, Apostolaki S and Danciu L (2024) Seismic hazard zonation map and definition of seismic actions for Greece in the context of the ongoing revision of EC8. *Bulletin of Earthquake Engineering* 22(8): 3753–3792.
- Porter KA (2003) An overview of PEER's performance-based earthquake engineering methodology. In: *Ninth international conference on applications of statistics and probability in Civil Engineering ICASP9*, San Francisco, CA, 6–9 July. Available at: <http://courses.washington.edu/cee518/Porter.pdf>
- Psyras N, Kwon O, Gerasimidis S and Sextos A (2019) Can a buried gas pipeline experience local buckling during earthquake ground shaking? *Soil Dynamics and Earthquake Engineering* 116: 511–529.
- Psyras NK and Sextos AG (2018) Safety of buried steel natural gas pipelines under earthquake-induced ground shaking: A review. *Soil Dynamics and Earthquake Engineering* 106: 254–277.
- Roche T, Merz K, Burger P, Doran G, McCabe E, Nitta S and Ostrom D (1995) Industry. *Earthquake Spectra* 11(2\_suppl): 245–285.
- RTI International (2015) *Emissions Estimation Protocol for Petroleum Refineries*. Available at: [https://www.epa.gov/sites/production/files/2020-11/documents/protocol\\_report\\_2015.pdf](https://www.epa.gov/sites/production/files/2020-11/documents/protocol_report_2015.pdf)
- Silva V, Akkar S, Baker J, Bazzurro P, Castro JM, Crowley H, Dolšek M, Galasso C, Lagomarsion S, Monteiro R, Perrone D, Pitilakis K and Vamvatsikos D (2019) Current challenges and future trends in analytical fragility and vulnerability modeling. *Earthquake Spectra* 35(4): 1927–1952.
- Steinberg LJ and Cruz AM (2004) When natural and technological disasters collide: Lessons from the Turkey Earthquake of August 17, 1999. *Natural Hazards Review* 5(3): 121–130.
- Vamvatsikos D and Cornell CA (2002) Incremental dynamic analysis. *Earthquake Engineering & Structural Dynamics* 31(3): 491–514.
- Vamvatsikos D and Cornell CA (2005) Developing efficient scalar and vector intensity measures for IDA capacity estimation by incorporating elastic spectral shape information. *Earthquake Engineering and Structural Dynamics* 34(13): 1573–1600.
- Vasquez Munoz LE and Dolšek M (2023) A risk-targeted seismic performance assessment of elephant-foot buckling in walls of unanchored steel storage tanks. *Earthquake Engineering and Structural Dynamics* 52(13): 4126–4147.
- Vathi M and Karamanos SA (2018) A simple and efficient model for seismic response and low-cycle fatigue assessment of uplifting liquid storage tanks. *Journal of Loss Prevention in the Process Industries* 53: 29–44.
- Vathi M, Karamanos SA, Kapogiannis IA and Spiliopoulos KV (2017) Performance criteria for liquid storage tanks and piping systems subjected to seismic loading. *Journal of Pressure Vessel Technology* 139(5): 051801.
- Wieschollek M, Kopp M, Hoffmeister B and Feldmann M (2011) Seismic design of spherical liquid storage tanks (COMPdyn 2011). In: *ECCOMAS Thematic Conference—COMPdyn 2011: 3rd international conference on computational methods in structural dynamics and earthquake engineering: An IACM Special Interest Conference, Programme, Corfu, 26–28 May*.
- Woessner J, Laurentiu D, Giardini D, Crowley H, Cotton F, Grünthal G, Valensise G, Arvidsson R, Basili R, Demircioglu MB, Hiemer S, Meletti C, Musson RW, Rovida AN, Sesetyan K and Stucchi M and The SHARE Consortium (2015) The 2013 European Seismic Hazard Model: Key components and results. *Bulletin of Earthquake Engineering* 13(12): 3553–3596.

- Xie Q, He C, Yang Z and Xue S (2019) Influence of flexible conductors on the seismic responses of interconnected electrical equipment. *Engineering Structures* 191: 148–161.
- Xu S, Wang Y and Feng X (2020) Plant layout optimization with pipe rack and frames. *Chemical Engineering Transactions* 81: 265–270. DOI:10.3303/CET2081045.
- Yoshida S (2014) Review of earthquake damages of aboveground storage tanks in Japan and Taiwan. In: *ASME 2014 pressure vessels and piping conference*, Anaheim, CA, 20–24 July.
- Zareian F, Aguirre C, Beltrán JF, Cruz E, Herrera R, Leon R, Millan A and Verdugo A (2012) Reconnaissance report of Chilean industrial facilities affected by the 2010 Chile offshore Bio-Bio earthquake. *Earthquake Spectra* 28(S1): S513–S532.
- Zhang Z, Park J, Kwon O-S, Sextos A, Strepelias E, Stathas N and Bousias S (2021) Hybrid simulation of structure-pipe-structure interaction within a gas processing plant. *Journal of Pipeline Systems Engineering and Practice* 12(2): 04020073.